Electronic Supplementary Material (ESI) for Physical Chemistry Chemical Physics.


# A Combined Optical and EPR Spectroscopy Study: Azobenzene-Based Biradicals as Reversible Molecular Photoswitches

Eva A. Jaumann, Sabrina Steinwand, Szabina Klenik, Jörn Plackmeyer, Jan W. Bats, Josef Wachtveitl, and Thomas F. Prisner

## Table of Content



## X-ray structure

The molecular structure of compound **2** obtained from X-ray diffraction data is shown in Figure S1. The molecule is centrosymmetric with a crystallographic inversion center at the midpoint of the central -N=N- double bond. The azobenzene group is planar (mean deviation from the best plane 0.008 Å). The five-membered pyrroline ring is also planar, but is bent by an angle of 21° out of the azobenzene plane due to crystal packing forces. The crystal packing is shown in Figure S2. The molecules are arranged in stacks parallel to the crystallographic a-axis direction. The interplanar distances between neighboring azobenzene groups in the stack is 3.58 Å which is a suitable distance for π···π interactions. The molecules are connected along the b-axis direction by a weak intermolecular $C_{pyrroline}$-H···O hydrogen bond with a H···O distance of 2.53 Å. The distance between the two unpaired electron spins (approximately center of the N-O bond of the nitroxides) for compound **2** is R = 2.25 nm (Compare R = 2.24 nm for compound **1** in the trans state).[1]

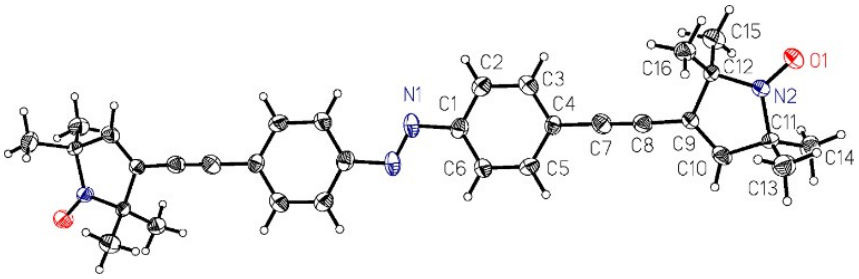


Figure S1: Molecular structure of compound **2** shown with 50% probability displacement ellipsoids. Unlabeled atoms are related to labeled atoms by an inversion center at the midpoint of the N=N-double bond.

## Crystal packing of compound 2

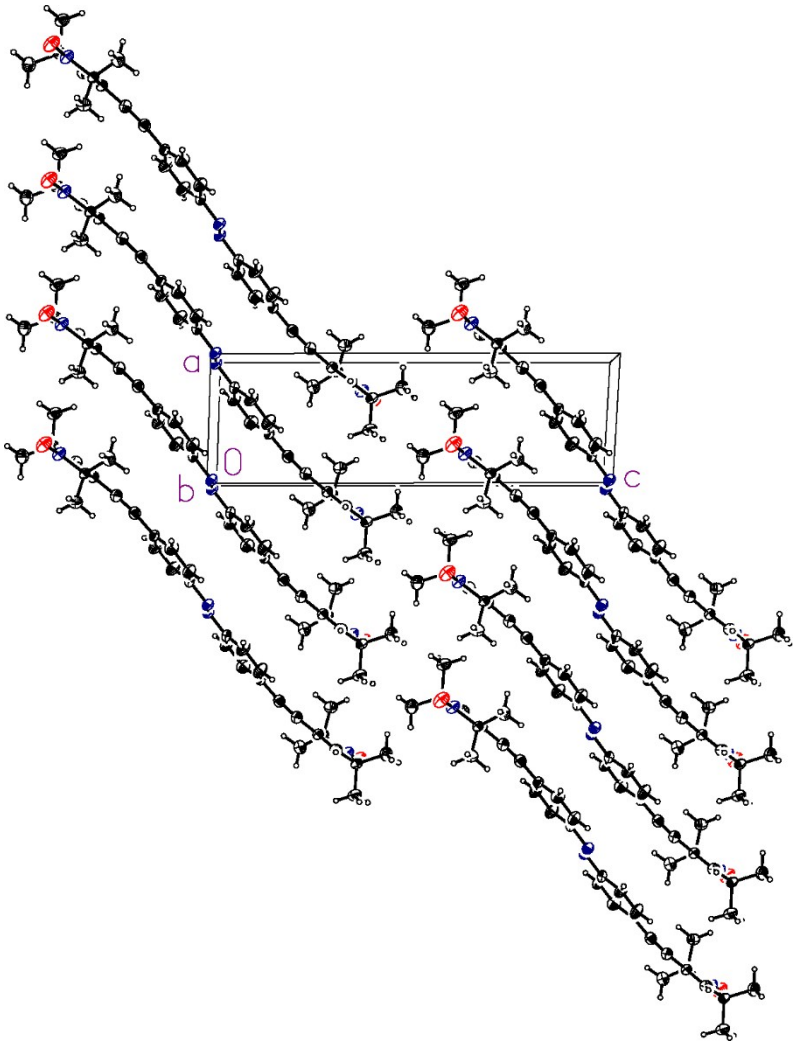


Figure S2: Crystal packing of compound **2** viewed along the b-axis direction.

## Vibrational structure

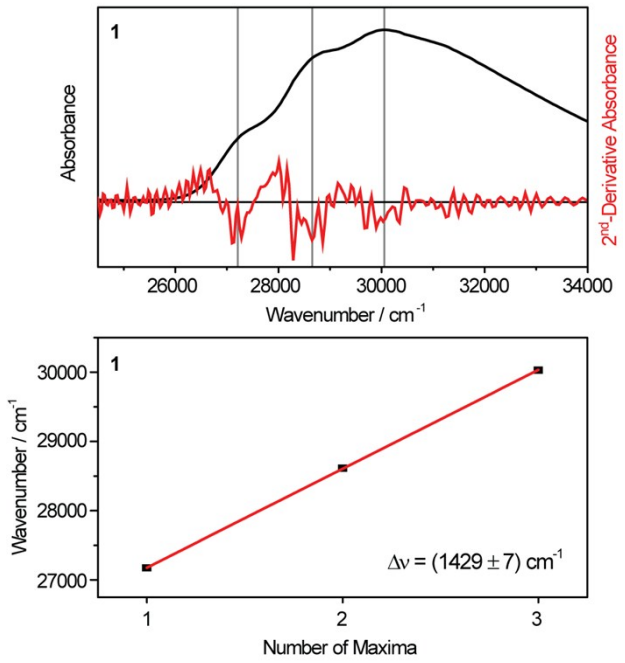


Figure S3: Vibrational structure of the *trans*-isomer of compound **1** ($2.8 \cdot 10^{-5}$ M) in toluene. Absorbance maxima are indicated by the second derivative of the absorbance spectrum (top). These maxima might be originated from a molecular vibration with a frequency of 1429 $cm^{-1}$ (bottom).

Referring to Figure 2, the *trans*-isomer of compound **1** shows a structured ππ*-absorbance band between 330 and 385 nm, which is contrast to compound **2**. Regarding these oscillations as vibrational structure, this structure refers to a vibrational frequency of 1429 $cm^{-1}$, which might correspond to the totally symmetric N=N stretching vibration of the *trans*-isomer. However, the origin of the structured absorbance bands of azobenzenes are still under debate.

## Quantum yield

Calculation of the quantum yield of the *trans*→*cis*- (ππ*) and *cis*→*trans*-isomerization (nπ*) was performed by using equation 1 with $m$ as the slope of the absorbance change of the photoproduct at the wavelength $\lambda_{pr}$ upon excitation [$s^{-1}$], $\varepsilon$ as the extinction coefficient at the wavelength $\lambda_{pr}$, $V$ as the sample volume [L], $d$ as the thickness of the sample [1 cm], $\lambda$ as the excitation wavelength [m], $P_0$ as the excitation power [W], $A_{prod,inf}$ as the product absorbance at long excitation duration (here neglected for compound **2**) and $A_{ex}$ as the initial absorbance at the excitation wavelength of the initial product, which was corrected by the amount of the photo-stationary state.

$$\Phi = \frac{m \cdot V \cdot N_A \cdot h \cdot c}{\varepsilon \cdot d \cdot \lambda \cdot P_0 \cdot \left(10^{-A_{prod,inf}} - 10^{-A_{ex}}\right)} \qquad (1)$$

Uncertainty analysis was performed by taking into account an error for the slope $m$ resulting from linear fit, for the volume $V$ (1%), for the power $P_0$ (5%), for the extinction coefficient $\varepsilon$

(5%), the product absorption $A_{prod,inf}$ (10% for *trans*→*cis*- and 50% for *cis*→*trans*-isomerization) and for the initial absorbance $A_{ex}$ (5%).

## Fatigue resistance

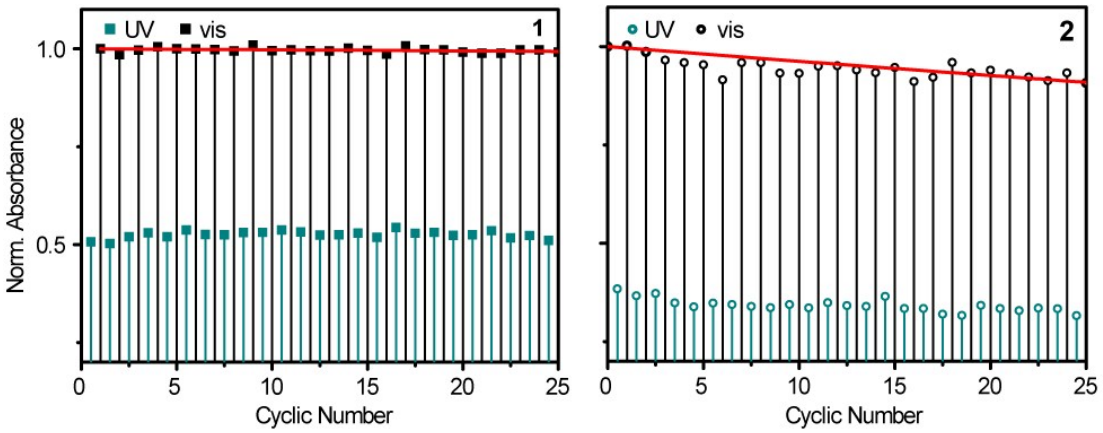


Figure S4: Fatigue resistance measurement of compound **1** ($\lambda$=333 nm) and compound **2** ($\lambda$=380 nm) in toluene, including fit analysis of degradation (*y* is 0.03% and 0.4%, respectively).

Fit analysis was performed using equation 2, which describes the degradation of each cycle.

$$y = (1 - x)^n \qquad (2)$$

with *x* as the degradation per cycle, *y* as the nondegraded fraction and *n* as the number of cycles.

## Room temperature cw-EPR simulations

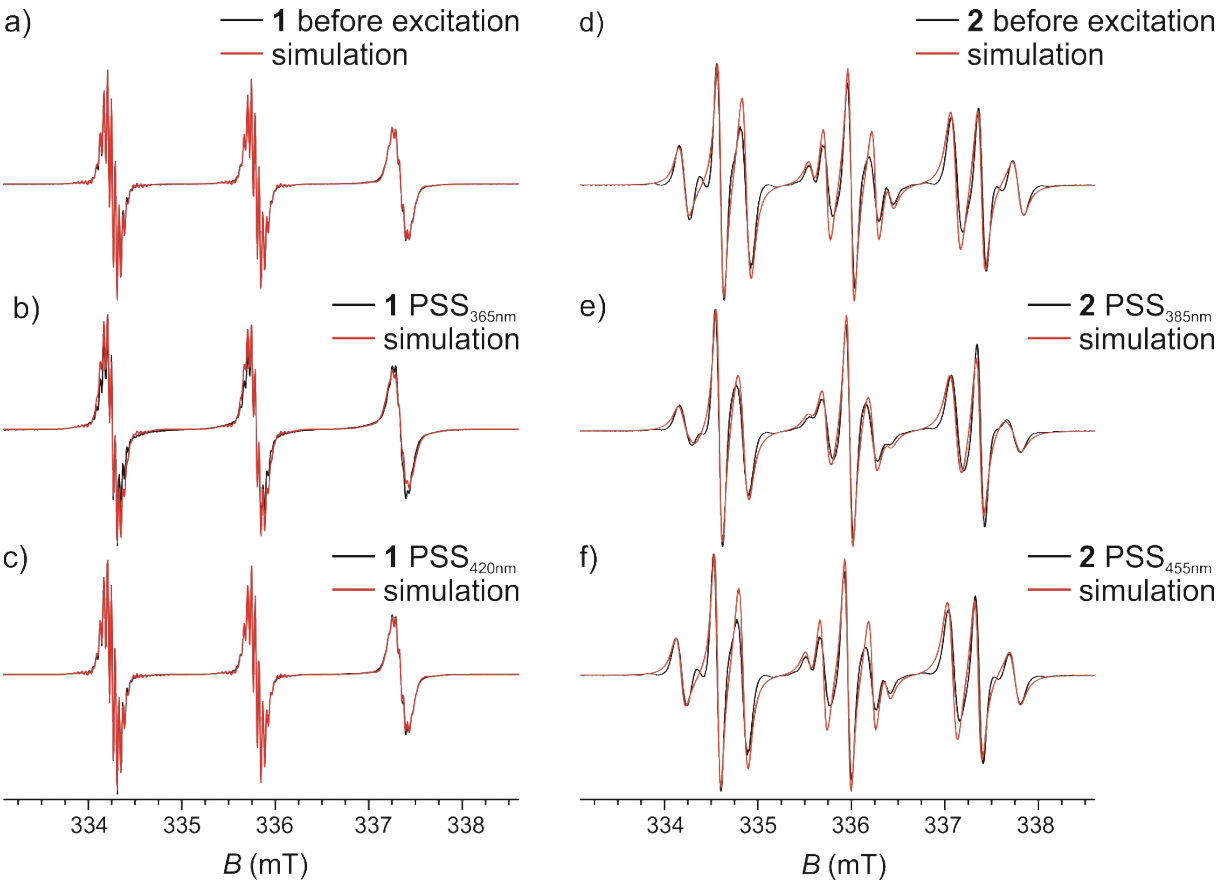


Figure S5: Simulations of the room temperature cw-EPR spectra of a), b) and c) compound **1** and d), e) and f) compound **2**. In figures S7 and S8 the experimental and simulated spectra are shown separately for better visualization.

The simulations were done with the EasySpin Package 5.0.22.[2] For compound **1** the function *garlic* for isotropic and fast-motion cw-EPR spectra was used. In Figure S5a) the experimental and simulated spectrum before any excitation of compound **1** is shown. For simplicity reasons, an isotropic rotational correlation time of 80 ps for the *trans*-isomer was assumed. After excitation with 365 nm, the experimental spectrum was simulated with 62% *cis*-isomer ($\tau_{corr}$ = 300 ps) and 38% *trans*-isomer (Figure S5b), according to the ratio obtained by optical spectroscopy. The *cis*→*trans*-isomerization, enabled by excitation with 420 nm leads to the experimental spectrum shown in Figure S5c) and was simulated assuming 100% *trans*-isomer.

The simulated spectra, also taking the hyperfine coupling to not only nitrogen, but also hydrogens and carbons into account are in good agreement with the experimental spectra.

Compound **1** has a long molecular axis. Therefore, its rotational correlation time should be better described by an anisotropic, axial diffusion tensor. Nevertheless, because the simulations using the simplifying assumption of an isotropic motion are already in very good agreement with the experimental spectra no attempt was made to determine the anisotropy

of the rotational diffusion tensor. Therefore, the rotational correlation time determined from the simulation should only be considered as a qualitative description.

Table 1: Hyperfine coupling constants, g values, linewidths and rotational correlation times for compound **1**. The two different sets of carbons can be explained with two neighboring Cα-atoms (C11 and C12) and four C-atoms (C13, C14, C15 and C16) in the methyl groups (see Figure S1 for labeling of the carbon atoms).

| | **compound 1 *trans*** | **compound 1 *cis*** |
|---|---|---|
| **[$g_{xx}$ $g_{yy}$ $g_{zz}$]** | [2.0089 2.0066 2.0022] | [2.0089 2.0066 2.0022] |
| **[$A_{xx}$ $A_{yy}$ $A_{zz}$]($^{14}$N)** | [19.2 19.2 91.5] MHz | [19.2 19.2 91.5] MHz |
| **12 × [$A_{xx}$ $A_{yy}$ $A_{zz}$]($^{1}$H)** | [1.1 1.1 1.1] MHz | [1.1 1.1 1.1] MHz |
| **2 × [$A_{xx}$ $A_{yy}$ $A_{zz}$]($^{13}$C)** | [17.7 17.7 17.7] MHz | [17.7 17.7 17.7] MHz |
| **4 × [$A_{xx}$ $A_{yy}$ $A_{zz}$]($^{13}$C)** | [13.1 13.1 13.1] MHz | [13.1 13.1 13.1] MHz |
| **linewidth [gaussian lorentzian]** | [0.028 0.01] mT | [0.028 0.01] mT |
| **$\tau_{corr}$** | 80 ps | 300 ps |

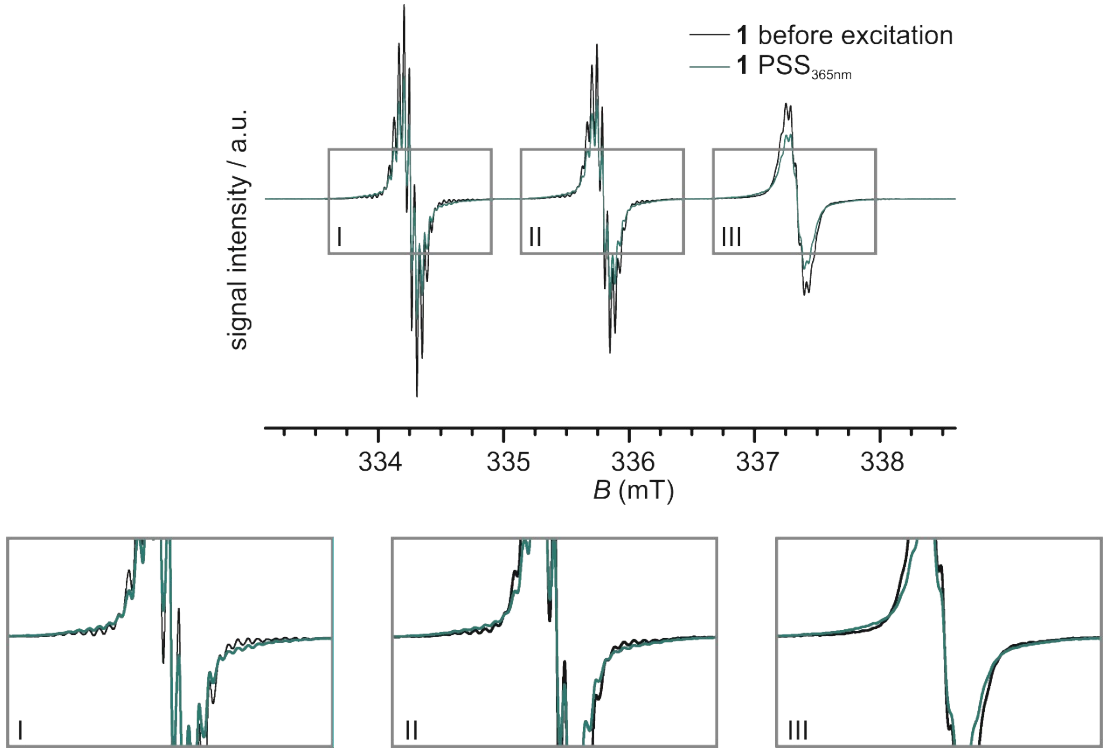


Figure S6: Comparison of the cw-EPR spectra of compound **1** before excitation (black, mainly *trans*-isomer) and after excitation with 365 nm (green, 62% *cis*-isomer and 38% *trans*-isomer). The magnified portions show a slight broadening of the lines in $PSS_{365nm}$.

Figure S6 shows the cw-EPR spectra of compound **1** before and after ($PSS_{365nm}$) excitation with 365 nm. Since the NO-NO distance is shorter in the *cis*- than in the *trans*-isomer, one may expect a broadening of the lines due to an increased dipolar coupling. With a rotational correlation time in the order of 80 ps and and NO-NO distance of 2.2 nm, the dipolar coupling for the *trans*-isomer is averaged out. For the *cis*-isomer with a shorter distance of r ≈ 1.6 nm and slower molecular tumbling rates of $\tau_{corr}$ = 300 ps the slight broadening of the lines, which

can be seen in the magnified portions of figure S6, could be caused by residual dipolar broadening. The effect is expected to be rather small, since the switching efficiency is not 100% , as determined by optical spectroscopy.

In contrast, the cw-EPR spectra of compound **2** show a more complex pattern, caused by the exchange coupling. In this case, the hydrogen hyperfine coupling is not resolved anymore. The line positions and pattern of the simulations match reasonable well (Figure S5d,e,f). To include not only the exchange coupling *J*, but also the a dynamic modulation of the exchange coupling with a frequency *R*, the simulations were performed as described by Dobryakov.[3] The ratios of *cis*- and *trans*-isomers were as obtained by optical spectroscopy: Before excitation 86% *trans*- and 14% *cis*-isomer (Figure S5d), after excitation (with 385 nm) 67% *cis*- and 33% *trans*-isomers (Figure S5e). After switching back (with 455 nm), the same ratio as before excitation was asumed (Figure S5f).

The simulations reveal an exchange coupling of $|J|$ = 19.3 MHz with an exchange frequency *R* = 0.8 MHz for the *trans*-isomer. The *cis*-isomer shows a slightly smaller exchange coupling $|J|$ = 16.0 MHz and an increased exchange frequency *R* = 2.8 MHz.

Table 2: Hyperfine coupling constants *A*(14N), magnitude of the exchange coupling $|J|$, exchange frequency *R* and an isotropic rotation correlation time of 100 ps for compound **2**.

| | **compound 2 *trans*** | **compound 2 *cis*** |
|---|---|---|
| ***A*($^{14}$N)** | 39.8 MHz | |
| $\tau_{corr}$ | 100 ps | |
| **$\|J\|$** | 19.3 MHz | 16.0 MHz |
| ***R*** | 0.8 MHz | 2.8 MHz |

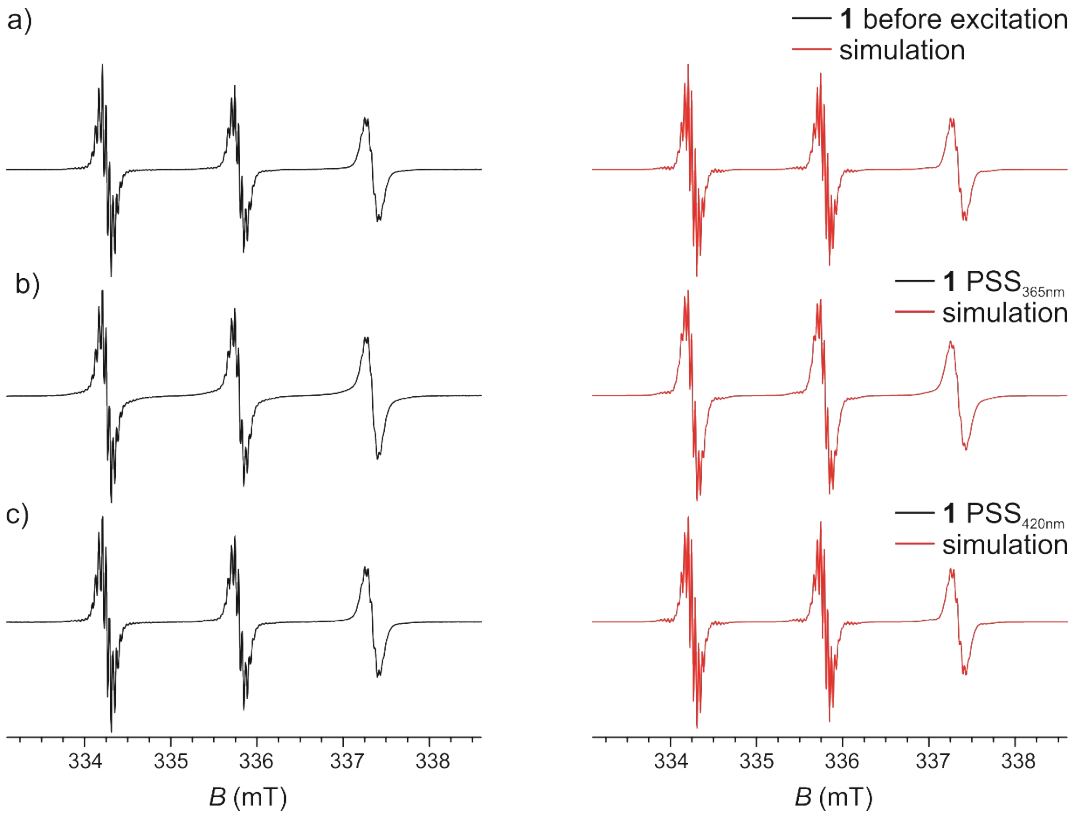


Figure S7: Experimental data (left side in black) and simulations (right side in red) of the room temperature cw-EPR spectra of compound **1** (see also figure S5 for the direct overlay). a) before light excitation b) after light excitation with 365 nm, c) after light excitation with 420 nm.

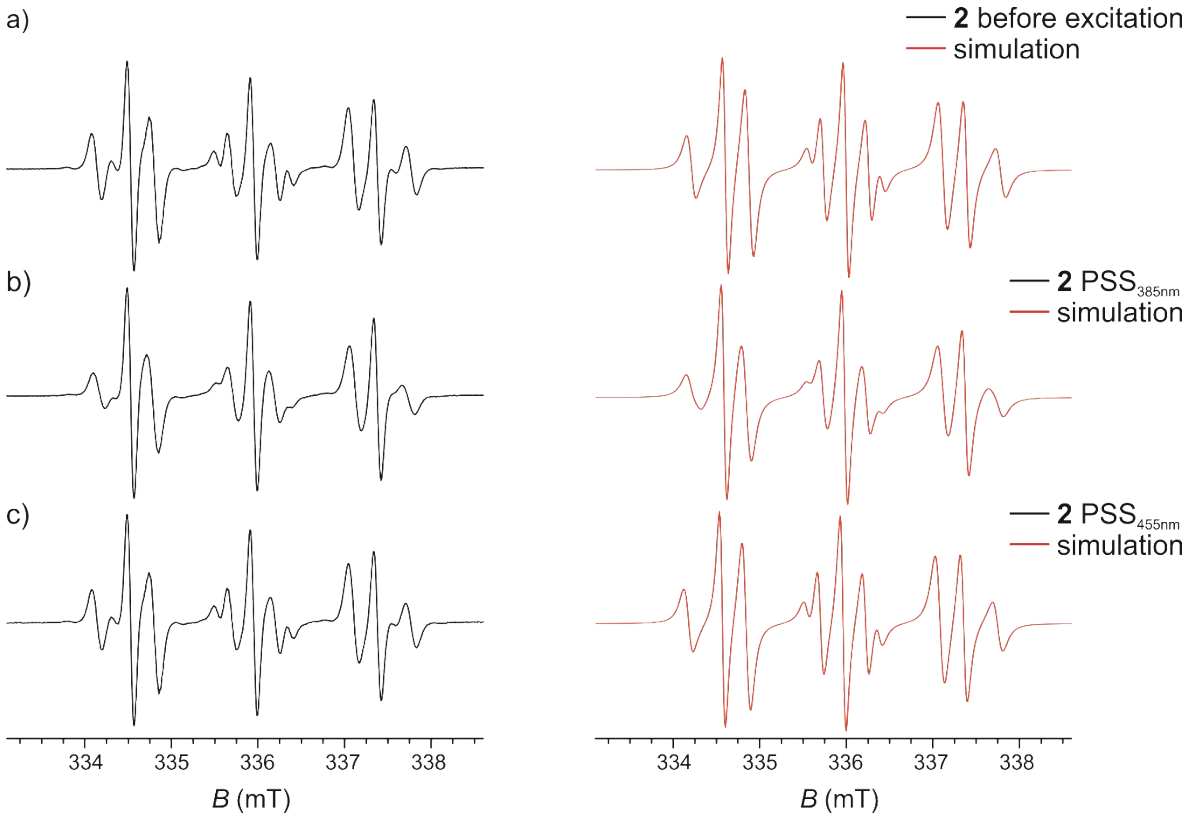


Figure S8: Experimental data (left side in black) and simulations (right side in red) of the room temperature cw-EPR spectra of compound **2** (see also figure S5 for the direct overlay). a) before light excitation b) after light excitation with 385 nm, c) after light excitation with 455 nm.

## PELDOR original data

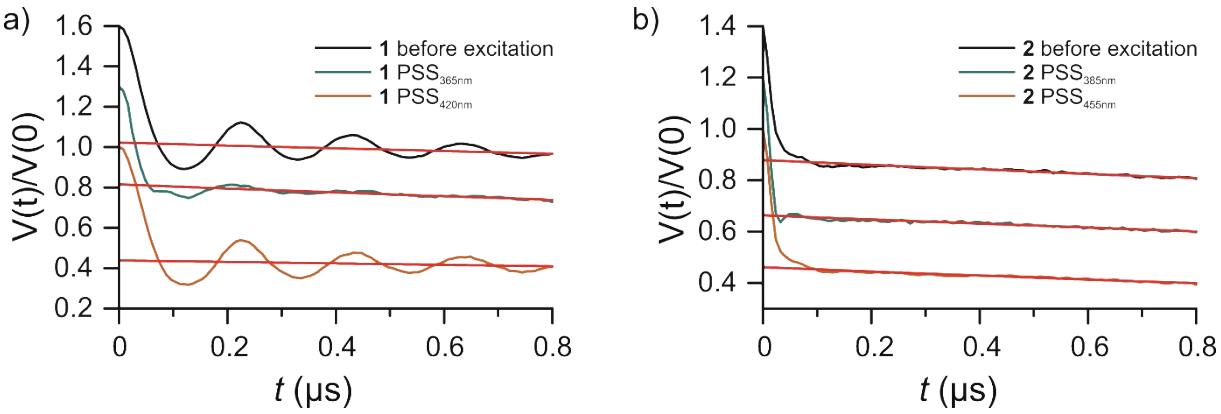


Figure S9: PELDOR time traces of compound **1** a) and compound **2** b). The red lines show the intermolecular exponential background functions.

# Simulation of Fourier Spectra

## 1. Compound 1

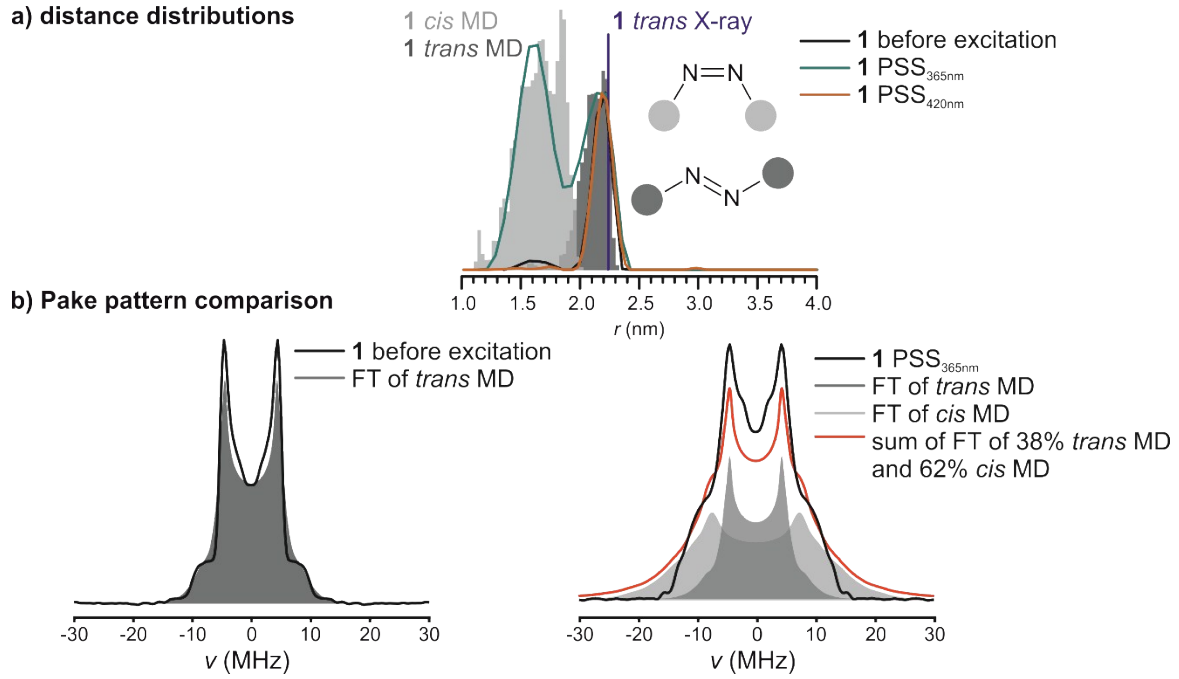


Figure S10: Simulation of the Fourier spectra of compound **1**. a) Calculated distance distributions from MD simulations (grey) and X-ray (purple line). b) Comparison of the experimental derived Pake pattern (black lines) with the calculated Pake pattern (gray areas) based on the MD simulated distance distributions. Left: before light excitation, Right: after light excitation with 365 nm.

The distance distributions extracted from the MD simulations compare rather well with the experimental distance distributions obtained from Tikhonov regularization of the PELDOR time traces (Figure S10a). Therefore, also the Pake pattern calculated from the MD distance distributions (Figure S10b) compare rather well, if the suppression of the larger frequency components of the cis-isomer by the used pulse lengths for the PELDOR sequence are taken into account. For $PSS_{365nm}$, a ratio of 38% *trans*- and 62% *cis*-isomers was assumed, as obtained by optical spectroscopy. Because the short distances for the *cis*-isomer are at the lower limit of the PELDOR method, an exact determination of the ratio between *trans*- and *cis*-isomer is not possible from the PELDOR data.

## 2. Compound 2

**a) distance distributions**

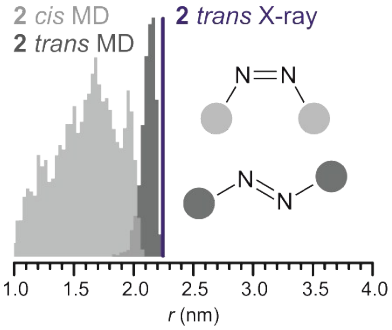


**b) simulation of Fourier spectra**

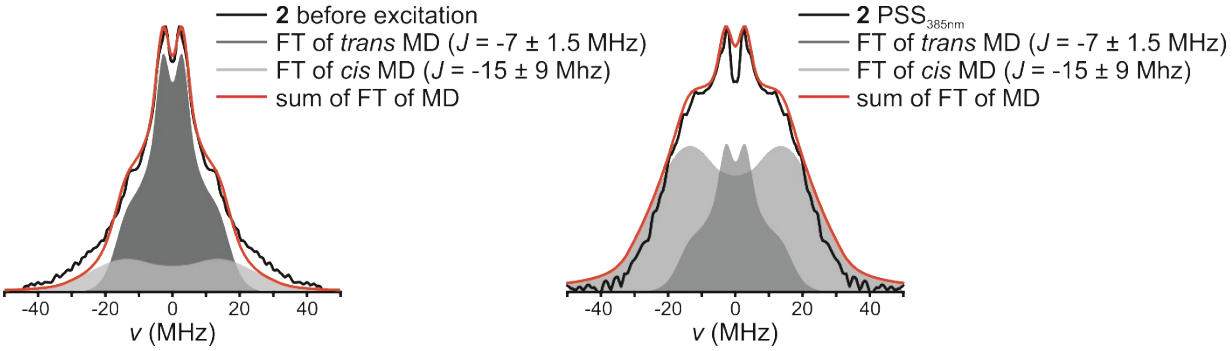


Figure S11: Simulations (red) of the experimental (black) Fourier spectra of compound **2**. a) Calculated distance distributions from MD simulations (grey) and X-ray (purple). b) Deconvolution of the Pake pattern with ferromagnetic exchange coupling. The simulation was performed with $r_{trans}$ = 2.1 ± 0.2 nm, $r_{cis}$ = 1.9 ± 1 nm, $J_{trans}$ = -7 ± 1.5 MHz, $J_{cis}$=-15 ± 9 MHz (all assumed as Gaussian distributions).

Typically, the exchange coupling *J* is negligible in comparison with the anisotropic dipolar coupling and described as

$$\nu_D = D\left(1 - 3\cos^2\theta_{AB}\right) \qquad (3)$$

with the dipolar coupling constant *D*

$$D = \frac{\mu_0 g_A g_B \beta_e^2}{4\pi\hbar} \cdot \frac{1}{r_{AB}^3} \qquad (4)$$

$\mu_0$ is the vacuum permeability, $g_A$ and $g_B$ are the *g* values of the two spins A and B, $\beta_e$ the Bohr magneton, $r_{AB}$ the distance between the spins A and B and $\theta_{AB}$ the angle between $r_{AB}$ and the external magnetic field.

However, if the exchange coupling *J* is non-zero, the dipolar coupling will be calculated by using equation (5)

$$\nu_{AB} = \nu_D + J = \frac{\mu_0 g_A g_B \beta_e^2}{4\pi\hbar} \cdot \frac{1}{r_{AB}^3}\left(1 - 3\cos^2\theta_{AB}\right) + J \qquad (5)$$

The exchange coupling *J* is defined here *via* the Hamiltonian

$$\hat{H}_J = + J\hat{S}_A\hat{S}_B \qquad (6)$$

Therefore, a positive exchange coupling corresponds to an antiferromagnetic ground state whereas a negative exchange coupling indicates a ferromagnetic ground state.

Simulation of the Fourier-transform spectra of the PELDOR time traces taking a Gaussian distribution of exchange couplings $J_{cis}$ and $J_{trans}$ for both isomers into account are shown in Figure S11. Good agreement could be achieved under the assumption of a ferromagnetic exchange coupling of $J$=-7 MHz for the *trans*-isomer and a large distribution of $J$ values for the *cis*-isomer of compound **2**. This distribution $\Delta J$ can be explained by the flexibility of the molecules, where different molecular conformers existing in the frozen state have different exchange couplings, which is also seen in the distance distribution (especially for the *cis*-isomer). Nevertheless, because the real distribution shapes of the exchange coupling are not known, as the exact shape of the distance distributions *P(R)* for both states, the values have to be considered in the best case as qualitative. This might be reflected by the differences in the main value of $J$ obtained for the *trans* state from the RT cw-EPR spectra and the low-temperature Fourier-transform spectra.

As already mentioned for compound **1**, also the short distance for the *cis*-isomer of compound **2** is below the lower limit of the PELDOR method. Therefore, it is not possible to determine the ratio between the two isomers precisely from the PELDOR data.

## References


1 S. L. Bekö, S. D. Thoms and M. U. Schmidt, *Acta Crystallogr. Sect. C Cryst. Struct. Commun.*, 2013, **69**, 1513–1515.

2 S. Stoll and A. Schweiger, *J. Magn. Reson.*, 2006, **178**, 42–55.

3 S. N. Dobryakov, in *Bioactive Spin Labels*, 1992, pp. 215–225.